Published in final edited form as:
Neuropsychologia. 2013 August ; 51(9): . doi:10.1016/j.neuropsychologia.2013.05.025.

Interactions between reward and threat during visual processing

Kesong Hu[*], **Srikanth Padmala**[*], and **Luiz Pessoa**
Department of Psychology, University of Maryland, College Park, MD, USA

Abstract

Appetitive stimuli such as monetary incentives often improve performance whereas aversive stimuli such as task-irrelevant negative stimuli frequently impair performance. But our understanding of how appetitive and aversive processes *simultaneously* contribute to brain and behavior is rudimentary. In the current fMRI study, we investigated interactions between reward and threat by investigating the effects of monetary reward on the processing of task-irrelevant threat stimuli during a visual discrimination task. Reward was manipulated by linking fast and accurate responses to foreground stimuli with monetary reward; threat was manipulated by pairing the background context with mild aversive shock. The behavioral results in terms of both accuracy and reaction time revealed that monetary reward eliminated the influence of threat-related stimuli. Paralleling the behavioral results, during trials involving both reward and threat, the imaging data revealed increased engagement of the ventral caudate and anterior mid-cingulate cortex, which were accompanied by increased task-relevant processing in the visual cortex. Overall, our study illustrates how the *simultaneous* processing of appetitive and aversive information shapes both behavior and brain responses.

Keywords

reward; threat; fMRI; ventral caudate; anterior mid-cingulate cortex

1. Introduction

Both appetitive and aversive processes impact behavior. For example, positive incentives such as monetary reward improve performance across a diverse set of perceptual and cognitive tasks (Engelmann & Pessoa, 2007; Krebs et al., 2010; Savine et al., 2010; Shen & Chun, 2011). At the same time, task-irrelevant negative stimuli have detrimental effects on performance during related tasks (Dolcos & McCarthy, 2006; Erthal et al., 2005; Hartikainen et al., 2000; Padmala et al., 2011). Yet, the effects of appetitive and aversive processes on brain and behavior have been investigated largely in an independent fashion (but see Amemori & Graybiel, 2012; Park et al., 2011; Talmi et al., 2009; Choi et al., in press). Hence, our understanding of how appetitive and aversive processes *simultaneously* contribute to brain and behavior is rudimentary.

Corresponding author: Dr. Luiz Pessoa, Department of Psychology, University of Maryland, College Park, MD 20742, pessoa@umd.edu, Phone: 301-405-2423.
[*]These authors contributed equally to this work

Investigating this interaction is important for at least two reasons. First, whereas many brain regions have been traditionally linked to appetitive (Haber & Knutson, 2010; Schultz et al., 2000) or aversive (Craig, 2002; LeDoux, 2000) processing, it is increasingly clear that they are engaged during both (Bromberg-Martin et al., 2010; Mizuhiki et al., 2012; Salamone, 1994; Salzman et al., 2007). Hence, a deeper understanding of the function of these regions necessitates utilizing paradigms that simultaneously manipulate both dimensions. Second, this type of interaction is not hypothetical; in many real-life contexts, rewards and threats may have to be simultaneously considered during behavior. For example, a chimpanzee may be motivated to consume a juicy piece of fruit, but know that doing so may trigger being badly smacked by a higher-ranking male.

In a recent study (Choi, et al., in press), we unraveled extensive competitive interactions between appetitive and aversive processing. The interactions were observed during an anticipatory delay "state", namely, in the absence of an explicit stimulus. In the present study, the goal was to investigate interactions between appetitive and aversive processes during perceptual processing, in part to understand potential interactions. We used a factorial design and investigated the effects of monetary reward on the processing of task-irrelevant threat-related stimuli (Fig. 1). Participants performed a visual discrimination task involving a set of stimuli (say, houses) initially associated with reward and a set of stimuli (say, buildings) not associated with reward. Visual stimuli (that is, houses or buildings) were overlaid on task-irrelevant colored backgrounds that were previously linked to "threat" or "safe" contexts, respectively.

In a previous study, we showed that motivation is capable of influencing distractor processing by up-regulating attention when reward is at stake (Padmala & Pessoa, 2011). Participants were informed of the possibility of reward by a cue stimulus that preceded the target phase during which a Stroop-like interference stimulus was displayed. We proposed that, because reward enhanced attention, the influence of task-irrelevant distractors was reduced leading to decreased conflict during incongruent trials. The goal of the present study was to extend our understanding of the interactions between motivation and attention in two ways. First, we wished to test whether reward would counter the effect of a more powerful task-irrelevant stimuli, such as the one used here that had a history of being linked to aversive electrical stimulation. Second, whereas several neuroimaging studies have investigated how reward cues influence perceptual/cognitive processes, less is known when the impact of reward is *reactive* in nature – especially in the presence of emotional stimuli. Proactive processes that allow one to prepare thoughts and actions in advance based on expectations regarding the upcoming events would be engaged in the case where reward cues are shown in advance, but reactive processes would be engaged when the possibility of reward is not informed in advance of the task at hand (Kiss et al., 2009; Krebs et al., 2011; Kristjansson et al., 2010). This is the case of our visual discrimination task (Fig. 1), during which one of the stimulus categories (house or building) was reward relevant while the other was not. Probing this type of reactive processing (see also Krebs et al., 2011) is relevant because minimizing the influence of distracting information may benefit from an advance stimulus cue – and possibly the upregulation of *proactive* control processes. In all, our goal was to investigate how the simultaneous presence of appetitive and aversive stimuli affect brain and behavior.

2. Materials and Methods

2.1 Participants

Twenty-six volunteers (17 males, mean age = 21 years, range = 18-29 years, all right-handed) with normal or corrected-to-normal vision participated in this study. Based on self-report, all participants were in good health with no past history of neurological or psychiatric

disease. The study was approved by the Institutional Review Board of the University of Maryland, College Park, and all participants provided written informed consent before participating in the study.

2.2 Stimuli and behavioral paradigm

The experiment consisted of two phases: instructed fear conditioning phase (6 runs) and the discrimination task phase (6 runs). Participants completed instructed fear and discrimination task runs in alternating fashion starting with the instructed fear conditioning run.

During an instructed fear conditioning run, each trial started with a fixation display for 1000 msec and was followed by a colored (yellow or green) square for 800 msec (Fig. 1A). Participants were required to passively view these colored squares (no response was required). Each trial ended with a 2-6 sec (mean: 3 sec) blank display. Before the start of the experiment, participants were explicitly informed that there was a chance of receiving a mild aversive shock when one of the colored squares appeared (for example: yellow [CS+] and green [CS-]; counterbalanced across participants). Shocks (US) occurred in 50% of CS+ trials, but the probability was not informed to participants. The US was 500 msec in duration and was delivered after 300 msec from the onset of the CS+ stimulus and hence co-terminated with it. At the beginning of the first instructed fear conditioning run, to calibrate the intensity of the electric shock, each participant was asked to choose his/her own stimulation level, such that the stimulus would be “highly unpleasant but not painful”. At the start of subsequent instructed fear conditioning runs, participants were asked about the unpleasantness of the US and were asked to, if needed, re-calibrate it so that the shock would be still “highly unpleasant but not painful”. Shocks were administered with an electrical stimulator (Coulbourn Instruments, PA, USA) on the fourth (“ring”) and fifth (“pinky”) fingers of the non-dominant left hand. The first instructed fear conditioning run included 40 trials (CS-: 20; CS+: 10; CS+ with US: 10) and the subsequent instructed fear conditioning runs included 20 trials per run (CS-: 10; CS+: 5; CS+ with US: 5). Each instructed fear conditioning run started and ended with a 20 sec blank display to provide adequate baseline signal for the fMRI analysis. Participants were told to relax during these blank displays at the start and end of each run.

During a discrimination task run, each trial started with an initial fixation display for 1000 msec and was followed by a picture of a house or building image overlaid on a yellow or green background for 800 msec (Fig. 1B). These images were chosen because they strongly recruit portions of visual cortex, specifically parahippocampal gyrus (PHG). To make the house/building images more discriminable, we made sure that all building images contained a clear vertical elongation whereas house images lacked this type of asymmetry (example images shown in Fig. 1B). Finally, each trial ended with a 2-6 sec (mean: 3 sec) blank display. Before the start of the experiment, participants were explicitly informed that with one of the image categories (for example: house [reward] or building [no-reward]; counterbalanced across participants) they would have the chance of winning extra monetary reward (100% contingency, which was informed to participants) based on fast and accurate performance. Hence, there were four trial types in this phase (Fig. 1B), allowing us to investigate the interactions between *Reward* and *Threat*. Participants were asked to indicate “house” or “building” by pressing the index or middle finger button (counterbalanced across participants). The RT threshold to determine “fast” responses was set at 650 msec based on behavioral pilot data. On each reward trial, participants won $0.25 if they were both accurate and fast. They won $0.00 during error or slow trials. During no-reward trials, participants won $0.00 irrespective of their performance. A visual reward feedback display (2 sec duration always followed by 8-sec blank display) with cumulative earnings was provided after every 8 trials. Each discrimination task run consisted of 24 trials (6 per trial type), thus providing 36 trials per condition for the entire experiment. Importantly, no shocks were

delivered during discrimination task runs and participants were explicitly informed about this. Each discrimination task run also started and ended with a 20 sec blank display to provide adequate baseline signal for the fMRI analysis. As before, participants were told to relax during these blank displays at the start and end of each run.

During the initial anatomical scan (see below) participants performed a short reward "familiarization block" so as to experience the reward structure. During this block, participants performed the same discrimination task as described above, except that house/building images were overlaid on a black background; additionally, participants received reward feedback after each trail. On average, participants won $22 over the entire experiment.

For the presentation of visual stimuli and recording of participant's responses, Presentation software (Neurobehavioral Systems, Albany, CA, USA) was used. Skin conductance response (SCR) data were also collected using the MP-150 system (BIOPAC Systems, Inc., CA, USA) at a sampling rate of 250 Hz by using MRI-compatible electrodes attached to the index and middle fingers of the non-dominant left hand. Due to technical problems during data collection, SCR data from the first conditioning run were lost in two participants.

2.3 MR Data Acquisition

MR data were collected using a 3 Tesla Siemens TRIO scanner (Siemens Medical Systems, Erlangen, Germany) with a 32-channel head coil (without parallel imaging). The scanning session began with a high-resolution MPRAGE anatomical scan (TR = 1900 ms, TE = 2.32 ms, TI = 900 ms, 0.9 mm isotropic voxels). Subsequently, for each functional run, BOLD EPI volumes were acquired with a TR of 2500 and TE of 25 ms. Each volume consisted of 44 oblique slices with a thickness of 3 mm and an in-plane resolution of 3 × 3 mm (192 mm field of view). Slices were positioned approximately 30 degrees clockwise relative to the plane defined by the line connecting the anterior and posterior commissures, helping to decrease susceptibility artifacts at regions such as the orbitofrontal cortex and amygdala. For the first instructed fear conditioning run, 96 EPI volumes were recorded and during subsequent instructed fear conditioning runs 56 EPI volumes were recorded. In each of the discrimination task runs 72 EPI volumes were recorded.

2.4 General fMRI data analysis

Pre-processing was done using tools from the AFNI software package (Cox, 1996; http://afni.nimh.nih.gov/afni). The first 3 volumes of each functional run were discarded to account for equilibration effects. The remaining volumes were slice-time corrected using Fourier interpolation, such that all slices were realigned to the first slice to account for timing differences. Six-parameter rigid-body motion correction within and across runs was performed using Fourier interpolation (Cox & Jesmanowicz, 1999), such that all volumes were spatially registered to the first volume. To normalize the functional data to Talairach space (Talairach & Tournoux, 1988), initially, each subject's high-resolution MRPAGE anatomical volume was spatially registered to the so-called TT_N27 template (in Talairach space) using a 12-parameter affine transformation; the same transformation was then applied to the functional data. All volumes were spatially smoothed using a Gaussian filter with a full-width at half maximum of 6 mm (i.e., two times the voxel dimension). Finally, the signal intensity of each voxel was scaled to a mean of 100 (on a per run basis), which allowed the interpretation of the estimated regression coefficients in terms of percent signal change.

2.5 Voxelwise analysis

Each participant's fMRI data were analyzed using multiple regression with AFNI (Cox, 1996). For the instructed fear conditioning runs, there were two main event types in the design matrix: CS- and CS+ trials. CS+ trials with physical shock (US) were modeled separately using an additional regressor of no interest. Constant, linear, and quadratic terms were included for each run separately (as covariates of no interest) to model baseline and drifts of the MR signal. To account for the signal variance related to head motion, six estimated motion parameters were included as nuisance regressors in the model. No assumptions were made about the shape of the hemodynamic response function. Responses were estimated starting from picture onset to 15 sec using cubic spline basis functions. This method is closely related to the use of finite impulses ("stick functions"), a commonly employed technique that can be considered the simplest form of basis expansion. Cubic splines allow for a smoother approximation of the underlying responses, instead of the discrete approximation obtained by finite impulses. As an index of response strength, we used the estimated response at 5 sec time point after picture onset (as determined via the spline-based estimates) for each main event type.

For the discrimination task runs, there were a total of four main event types in the design matrix: no-reward and reward events, separately for the CS- and CS+ conditions. Both error and reaction time (RT) outlier trials were modeled separately using additional regressors of no interest (pooled over all four conditions). Reward feedback trials were modeled separately using an additional regressor of no interest. As before, constant, linear, and quadratic terms were included for each run separately (as covariates of no interest) to model baseline and drifts of the MR signal, and six estimated motion parameters were included as nuisance regressors in the model. No assumptions were made about the shape of the hemodynamic response function. Responses were estimated starting from picture onset to 15 sec using cubic spline basis functions. As an index of response strength, we used the estimated response at 5 sec time point after picture onset (as determined via spline-based estimates) for all four main event types.

2.6 Group analysis

Whole-brain voxelwise random-effects analyses were restricted to gray-matter voxels based on the FSL automated segmentation tool FAST (FMRIB's Automated Segmentation Tool; http://www.fmrib.ox.ac.uk/fsl/). For the instructed fear conditioning runs, we contrasted CS + vs. CS- conditions using a paired *t* test.

The central goal of the voxelwise analysis in the discrimination task was to define regions of interest (see below). However, for the sake of completeness, a voxelwise analysis was also performed and followed the same 2 *Reward* (reward, no-reward) × 2 *Threat* (CS+, CS-) repeated-measures ANOVA employed in the region of interest analysis.

The alpha-level for voxelwise statistical analysis was determined by simulations using the 3dClustSim program of the AFNI toolkit. For these simulations, the smoothness of the data in three directions was estimated using 3dFWHMx on the residual time series of gray-matter voxels in each participant and then averaged across participants (FWHMx = 8.62 mm; FWHMy = 8.33 mm; FWHMz = 7.75 mm). Based on a voxel-level uncorrected alpha of .001, simulations indicated a minimum cluster extent of 19 voxels for a cluster-level corrected alpha of .05.

2.7 Region of interest analysis

To enhance statistical power, we focused the discrimination task analysis on a set of regions of interest (ROIs) that were robustly activated by the task. ROIs were defined based on the

main effect of *Reward* or *Threat* at a cluster-level alpha value of < .05. Each activation cluster of the main effects themselves was defined as an individual ROI. Based on a priori hypotheses concerning the involvement of the parahippocampal gyrus (PHG) in scene processing, the right PHG ROI was selected based on the main effect of *Threat* at $p < .005$, uncorrected, and 30-voxel cluster extent. We adopted the selection criterion of main effects to determine ROIs, because it was statistically independent of the central goal of our analysis, that is, to probe the *Reward* by *Threat* interactions (see below) (Kriegeskorte et al., 2009; Vul et al., 2009). A representative time series for each ROI was then created by averaging the time series of all the gray matter voxels inside the ROI. Then, for each ROI, as in the whole-brain voxelwise analysis, deconvolution analysis was run on the representative time series data to estimate the hemodynamic response function of four main regressors of interest. Then, for each condition, we took the estimated response at 5 sec time point following picture onset as the index of response strength. Our central aim in this study was to assess the interactions between *Reward* and *Threat*. As such, for each ROI, response strength indices were submitted to a 2 *Reward* (reward, no-reward) × 2 *Threat* (CS+, CS-) repeated measures ANOVA.

2.8 Relationship between brain responses during the discrimination task

We investigated the relationship between brain responses of regions exhibiting significant *Reward* × *Threat* interactions. To do so, for each participant, we first created the fMRI interaction index ($[CS+ - CS-]_{REWARD} - [CS+ - CS-]_{NO\text{-}REWARD}$) for each ROI separately. Then, across participants, we investigated this interaction index between each pair of ROIs using robust regression (Wager et al., 2005). We employed iterative reweighted least squares (the robustfit function from Matlab, Mathworks, Natick, MA, USA), given that standard Pearson correlation is sensitive to even a few influential data points (Wilcox, 2005).

2.9 Relationship between brain responses and behavior during the discrimination task

To investigate the potential link between behavior and brain responses in the ROIs exhibiting significant *Reward* × *Threat* interactions, for each ROI, we ran an across-subject robust regression analysis between fMRI responses and RT scores. This analysis was done separately for CS+ and CS- conditions using the differential (reward minus no-reward trials) RT scores and corresponding differential fMRI signals.

2.10 Behavioral data analysis

For RT analysis, error trials (5.07%) and outlier trials (0.53%) with RT exceeding three standard deviations from the condition-specific mean were excluded. For each participant, mean RT and error rate data were determined as a function of *Reward* (CS+, CS-) and *Threat* (reward, no-reward) conditions. Analyses of variance (ANOVAs) were conducted on the mean RT and mean error rate data, with those variables as within-subject factors. The alpha-level adopted was .05.

2.11 Skin Conductance Response (SCR) analysis

Each participant's SCR data collected during instructed fear conditioning runs were initially smoothed with a median-filter over 50 samples (200ms) to reduce scanner-induced noise and resampled at 1 Hz. The pre-processed SCR data were then analyzed using multiple regression in AFNI (Cox, 1996). For related approaches see Bach et al. 2009 and Choi et al., 2012. As in the imaging data analysis, there were two main event types in the design matrix: CS- and CS+ trials. CS+ trials with shock (US) were modeled separately using an additional regressor of no interest. No assumptions were made about the shape of the SCR function. The average response to each trial type was estimated via deconvolution. Responses were estimated starting from picture onset to 15 sec post onset using cubic spline basis functions

(see fMRI analysis above for further discussion). Constant and linear terms were included for each run separately (as covariates of no interest) to model baseline and drifts of the SCR. For each event type, as an index of response strength, we used the mean of the estimated responses at 4 and 5 sec post picture onset (similar time range as used in the imaging data analysis). In order to equalize variance, response-strength indices were transformed by using a logarithm function (log[1+SCR]). Then, a paired t-test was run to contrast CS+ vs. CS- conditions.

3. Results

3.1 Instructed fear conditioning

To verify the effectiveness of our instructed fear conditioning procedure, we contrasted SCR responses during instructed fear conditioning runs for CS+ and CS- trials using a paired *t*-test. As shown in Figure 2A, SCR responses were stronger during the CS+ relative to CS- condition ($t_{25} = 2.56$, $p = .017$), indicating that our instructed fear conditioning procedure was successful.

In terms of brain responses, during instructed fear conditioning runs, stronger responses during CS+ relative to CS- trials were observed in the bilateral anterior insula and right inferior frontal gyrus (Fig. 2B; Table 1), consistent with findings reported in instructed fear conditioning studies (Mechias et al., 2010). We note that, although a lack of a conditioning effect in the amygdala is somewhat surprising, it has been observed that not all instructed fear conditioning studies detect a significant effect in the amygdala (Mechias et al., 2010).

3.2 Discrimination task: Behavioral results

Mean RT data were evaluated according to a 2 *Reward* (no-reward, reward) × 2 *Threat* (CS-, CS+) repeated-measures ANOVA (Fig. 3A). The main effect of *Reward* was significant ($F_{1, 25} = 47.71$, $p < .001$). Mean RT was faster during the reward (465 msec) compared to the no-reward condition (511 msec), demonstrating the effectiveness of the reward manipulation. The main effect of *Threat* was marginally significant ($F_{1, 25} = 3.29$, $p = .082$), such that RTs during the CS+ condition (490 msec) were numerically slower compared to the CS- condition (486 msec). Critically, the *Reward* × *Threat* interaction was significant ($F_{1, 25} = 11.18$, $p = .003$), such that the slower RT during CS+ compared to CS- trials during the no-reward condition (14 msec) was reduced during the reward condition (-5 msec).

Because we observed a main effect of *Reward* such that the overall RT was faster during the reward condition, it is conceivable that the reduced threat interference during the reward condition could be due to overall faster RTs (faster RTs would leave less “room” for interference). Therefore, we calculated a ratio-based index of threat interference (CS+/CS-) separately for the reward and no-reward conditions. A comparison of the two via a paired *t* test revealed a significant difference ($t(25) = 3.31$, $p = .003$), supporting the inference of reduced threat interference during the reward condition. This analysis demonstrates that the reduction of threat interference during reward was not simply due to overall faster RTs.

The 2 *Reward* × 2 *Threat* repeated-measures ANOVA on mean error rate data (Fig. 3B) also revealed a main effect of *Reward* ($F_{1, 25} = 8.43$, $p = .008$), such that error rate was smaller during reward (2.9%) compared to no-reward (7.2%). The main effect of *Threat* was marginally significant ($F_{1, 25} = 3.42$, $p = .076$). Notably, a significant *Reward* × *Threat* interaction effect was detected ($F_{1, 25} = 6.95$, $p = .014$). As with the RT data, the increased error rate during CS+ compared to CS- trials during no-reward (3.5%) was significantly reduced during reward (-1.0%).

3.3 Discrimination task: fMRI results

To increase statistical power, interactions between *Reward* and *Threat* were probed across ROIs that exhibited main effects (Fig. 4; Table 2). Consistent with the literature, in the voxelwise analysis, a significant main effect of *Reward* was observed in several subcortical and cortical regions including bilateral ventral caudate extending into nucleus accumbens, right thalamus, middle frontal gyrus, bilateral anterior insula, and medial prefrontal cortex. In all these regions, responses were stronger during reward compared to no-reward conditions. Significant main effects of *Threat* were observed in left middle temporal gyrus and left superior temporal gyrus. In these two regions, responses during the CS+ condition were stronger compared to the CS-condition.

The response estimates from these ROIs (including the right PHG ROI that was defined based on the main effect of *Threat*; see *Methods*) were submitted to a 2 *Reward* (no-reward, reward) × 2 *Threat* (CS-, CS+) repeated-measures ANOVA. Significant *Reward* × *Threat* interactions were detected in the right ventral caudate ($F_{1, 25} = 6.43$, $p = .018$; Fig. 5A), right anterior mid-cingulate cortex ($F_{1, 25} = 5.58$, $p = .026$; Fig. 5B), and right PHG ($F_{1, 25} = 6.27$, $p = .019$; Fig. 5C). In all these three regions, CS+ vs. CS- responses were stronger during reward compared to no-reward. Put another way, reward vs. no-reward responses were stronger during CS+ compared to CS- condition.

For completeness, we also investigated the *Reward* × *Threat* interactions over the whole brain. In this voxelwise analysis, significant interaction effects were detected in the right middle occipital gyrus only (peak voxel: x = 32; y = -79; z = 8; $F(1,25) = 36.98$).

3.4 Relationship between brain regions

The three regions shown in Figure 5 exhibited significant interaction scores. We reasoned that if they were engaged during the task as a "functional circuit", interaction "scores" ($[CS+ - CS-]_{REWARD} - [CS+ - CS-]_{NO\text{-}REWARD}$) across participants should be positively related between region pairs (for related approaches, see D'Ardenne et al., 2008; Padmala and Pessoa, 2011). A robust regression analysis using fMRI "interaction scores" of ROIs exhibiting significant *Reward* × *Threat* interactions, revealed a significant positive linear relationship between right ventral caudate and right PHG (robust $R^2 = 0.37$, $p = .004$; Fig. 6A) and between right anterior mid-cingulate cortex and right PHG (robust $R^2 = 0.27$, $p = .009$; Fig. 6B).

3.5 Relationship between brain responses and behavior

We further evaluated the link between brain responses in the regions of Figure 5 and behavior. A robust regression analysis linking brain responses and behavioral data revealed a significant negative linear relationship between differential (reward minus no-reward trials) RT scores during CS+ condition and corresponding differential fMRI signals in right ventral caudate (robust $R^2 = 0.41$, $p = .0004$; Fig. 7A). This suggests that participants with stronger responses during reward (relative to no-reward) trials in the right ventral caudate exhibited faster RT responses. This observed relationship was specific to the CS+ condition, as it was not observed during the CS- condition (robust $R^2 = 0.02$, $p = .508$).

3.6 Discrimination task: Amygdala ROI analysis

In the above analyses, we did not observe significant results in the amygdala. But given the theoretical importance of the amygdala in emotional processing, we conducted an additional ROI analysis to probe the signals in this area. Left and right amygdala ROIs were defined based on anatomy using the Talairach atlas provided with the AFNI package. In each ROI, a representative time series was created by averaging the pre-processed time series from all the gray-matter voxels within the anatomically defined amygdala ROI. Then, for each ROI,

as in the whole-brain voxelwise analysis, deconvolution analysis was run on the representative time series data to estimate the hemodynamic response function of four main regressors of interest. As before, for each condition, we used the estimated response at 5 sec following picture onset as the index of response strength. A 2 × 2 repeated-measures ANOVA was then run. The main effect of *Threat* was marginally significant bilaterally (Table 3), such that responses during CS+ trials were numerically greater compared to CS- trials. Neither a main effect of *Reward* nor a *Reward* × *Threat* interaction was detected.

4. Discussion

In this study, we investigated the interactions between reward and threat on brain and behavior during a visual discrimination task. Reward was manipulated in a *reactive* fashion by linking the task-relevant stimulus categories to reward or no-reward, whereas threat was manipulated using task-irrelevant backgrounds that were previously paired or not paired with aversive electrical stimulation.

Behaviorally, an unspecific effect of reward was observed in that RTs were faster during reward vs. no-reward conditions. This general "activation" effect is not surprising. Importantly, however, a reward by threat interaction was present, such that the slowing of RT by irrelevant threat stimuli that was observed during no-reward was *eliminated* during reward. Recently, several studies have reported specific effects of motivation during diverse perceptual and cognitive tasks (Engelmann & Pessoa, 2007; Krebs, et al., 2010; Savine, et al., 2010; Shen & Chun, 2011). In a recent fMRI study, we showed that monetary reward cues presented prior to the task phase reduced both interference and facilitation behavioral scores in a response conflict task, suggesting that motivation reduced the influence of task-irrelevant (neutral) words (Padmala & Pessoa, 2011). In another recent behavioral study, the authors manipulated motivation in a reactive fashion by associating a subset of colors in a color-word Stroop task with monetary reward; they reported reduced interference from task-irrelevant (neutral) words when the task-relevant colors were associated with reward (Krebs, et al., 2010). The behavioral results in our current study extend these past investigations by showing that monetary reward manipulated in a reactive fashion reduced the interference of potent task-irrelevant threat stimuli.

In terms of the brain, we observed a main effect of reward in the ventral caudate extending into nucleus accumbens and the midbrain, two brain regions centrally involved in reward-related processing (Delgado, 2007; Haber & Knutson, 2010; Schultz, et al., 2000). In addition to these subcortical sites, cortical areas also exhibited a main effect, including inferior parietal lobule, anterior and mid-cingulate cortices, middle frontal gyrus, and anterior insula. All these cortical regions have been reported to be involved in reward processing (Leon & Shadlen, 1999; Liu et al., 2011; Mohanty et al., 2008; Platt & Glimcher, 1999; Shidara & Richmond, 2002; Shima & Tanji, 1998). Interestingly, we did not observe the main effect of reward in the frontal eye field, a key node of the dorsal attention network (Corbetta & Shulman, 2002) that is engaged when reward is cued in advance of task execution (Engelmann et al., 2009; Harsay et al., 2011; Roesch & Olson, 2003). Both in the present study where reward was manipulated in a reactive fashion, and in previous studies where it was cued in advance, the ventral caudate and midbrain were engaged by reward. We thus propose that these *evaluative* areas interact with different attentional regions depending on the context in which reward may be attained.

A central objective of this study was to probe interactions between reward and threat processing. These were observed in the right ventral caudate, right anterior mid-cingulate cortex, and right PHG. The right PHG is an area that is strongly recruited by visual stimuli of "scenes" or "places" (Epstein et al., 1999). Response strength in this area was comparable

for all conditions, except for the reward-threat condition, during which responses were increased. If we consider PHG responses as an index of the strength of scene processing, it is possible that, during the reward-threat condition, increased scene-related processing occurred, perhaps allowing participants to reduce the interference from the threat background. In other words, given the potential for reward, participants enhanced task-relevant processing especially when the irrelevant threat background occurred so as to attain the potential reward.

An interaction pattern was also detected in the right ventral caudate and right anterior mid-cingulate cortex. Here, both ventral caudate and anterior mid-cingulate cortex exhibited an interaction pattern such that the largest response was observed during the reward-plus-threat condition. Krebs et al. (2012) observed interactions between reward and task difficulty (both signaled by a cue stimulus) in a set of brain regions comprising the midbrain, caudate nucleus, thalamus, and anterior mid-cingulate cortex. The authors suggested that the interaction may have reflected additional “resource recruitment”. Although speculative, it is possible that something similar took place in the present task. In other words, during trials involving both reward and threat, additional resources might have been garnered when the task was more demanding due to the distracting nature of the threat-related background.

In the context of the ongoing discussion, it is noteworthy that striatal regions play an important role in the allocation of resources devoted to actions (Boehler et al., 2011; Salamone et al., 2009). It has been proposed that dopamine-related circuits in the striatum facilitate the *reallocation* of limited processing capacity toward unexpected events of behavioral significance, including rewarding ones (Redgrave & Gurney, 2006; Redgrave et al., 1999). Thus, instead of simply providing a “reward signal,” striatal activation drives the redistribution of available resources to salient events whose processing is then prioritized (see also Horvitz 2000; Zink et al. 2004). In our data, we suggest that this was manifested not only in the increased responses in the ventral caudate during conditions involving reward (that is, a main effect of reward), but also in the reward by threat interaction pattern. Furthermore, across participants, the strength of the interaction in the ventral caudate was correlated with that of the PHG, consistent with the idea that increased resource recruitment was paralleled by enhanced visual responses to task-relevant scenes during reward-threat trials. The relationship between the responses of ventral caudate and PHG is broadly consistent with findings of earlier studies, where increased functional connectivity between subcortical and cortical regions was observed (Camara et al., 2008; Harsay, et al., 2011). We note, however, that evidence in terms of increased psycho-physiological interactions was not detected in the present study.

To investigate the link between brain and behavior, we evaluated the relationship between differential RT scores (reward minus no-reward trials) and corresponding differential fMRI responses during threat. We observed an inverse linear relationship between RT scores and fMRI responses in the right ventral caudate. Along the lines of the previous paragraph, we tentatively interpret these findings as suggesting that the potential for reward during reward-plus-threat trials increased resource recruitment, thereby leading to faster RTs (and increased likelihood of reward).

We observed only a marginally significant main effect of *Threat* in the amygdala (with no interaction effect). If, in the context of our task, amygdala responses are considered as an index of the strength of emotional processing, these results suggest that the neural processing of threat distractors was not influenced by reward. Instead, reward increased the responses to task-*relevant* stimuli when faced with threat distractors. This observed pattern of results is different from that of our previous study, where we reported reduced processing of (neutral) distractor words in the left fusiform gyrus during reward conditions (Padmala &

Pessoa, 2011). This difference could be due to at least two factors. First, the processing of task-*irrelevant* aversive or negative stimuli is prioritized during low-demand task conditions (Pessoa, 2005) and hence not strongly influenced by reward. Second, in the current study, reward was manipulated in a *reactive* fashion, whereas it was manipulated in a *proactive* fashion in the earlier study.

We recently reported *competition* during the anticipation of reward *and* threat at multiple brain sites, including midbrain, striatum, anterior insula, and prefrontal cortex (Choi, et al., in press). In the study, stimulus-*independent* responses related to anticipation of reward were reduced during threat and stimulus-*independent* responses related to the anticipation of threat were reduced during reward. The results from the current study extend these neuroimaging findings to conditions involving interactions between appetitive and aversive processes that are stimulus *dependent*.

In conclusion, using a factorial design, we investigated interactions between the processing of reward and threat. Our behavioral results revealed that the influence of task-irrelevant threat stimuli was eliminated during the processing of reward-associated stimuli. In line with the behavioral findings, the imaging data revealed increased engagement of the ventral caudate and anterior mid-cingulate cortex, which was accompanied by increased task-relevant processing to scenes/places in the PHG during conditions involving both reward and threat. Overall, our study revealed how the *simultaneous* processing of appetitive and aversive information shapes both behavior and brain responses in ways that are only now being unraveled.

Acknowledgments

We acknowledge the National Institute of Mental Health for support for this work (award 1R01 MH071589). We also thank Philip Spechler for assistance with subject recruitment and data collection.

References

Amemori K, Graybiel AM. Localized microstimulation of primate pregenual cingulate cortex induces negative decision-making. Nature Neuroscience. 2012; 15(5):776–785.

Bach DR, Flandin G, Friston KJ, Dolan RJ. Time-series analysis for rapid event-related skin conductance responses. Journal of Neuroscience Methods. 2009; 184(2):224–234.10.1016/j.jneumeth.2009.08.005 [PubMed: 19686778]

Boehler CN, Hopf JM, Krebs RM, Stoppel CM, Schoenfeld MA, Heinze HJ, Noesselt T. Task-load-dependent activation of dopaminergic midbrain areas in the absence of reward. Journal of Neuroscience. 2011; 31(13):4955–4961.10.1523/JNEUROSCI.4845-10.2011 [PubMed: 21451034]

Bromberg-Martin ES, Matsumoto M, Hikosaka O. Dopamine in motivational control: rewarding, aversive, and alerting. Neuron. 2010; 68(5):815–834. [PubMed: 21144997]

Camara E, Rodriguez-Fornells A, Münte TF. Functional connectivity of reward processing in the brain. Frontiers in Human Neuroscience. 2008; 2

Choi JM, Padmala S, Pessoa L. Impact of state anxiety on the interaction between threat monitoring and cognition. NeuroImage. 2012; 59(2):1912–1923.10.1016/j.neuroimage.2011.08.102 [PubMed: 21939773]

Choi JM, Padmala S, Spechler P, Pessoa L. Pervasive competition between threat and reward in the brain. Social cognitive and affective neuroscience. in press. 10.1093/scan/nst053

Corbetta M, Shulman GL. Control of goal-directed and stimulus-driven attention in the brain. Nature Reviews Neuroscience. 2002; 3(3):201–215.

Cox RW. AFNI: Software for analysis and visualization of functional magnetic resonance neuroimages. Computers and Biomedical Research. 1996; 29:162–173. [PubMed: 8812068]

Cox RW, Jesmanowicz A. Real-time 3D image registration for functional MRI. Magnetic Resonance in Medicine. 1999; 42:1014–1018. [PubMed: 10571921]

Craig AD. How do you feel? Interoception: the sense of the physiological condition of the body. Nature Reviews Neuroscience. 2002; 3(8):655–666.

D'Ardenne K, McClure SM, Nystrom LE, Cohen JD. BOLD responses reflecting dopaminergic signals in the human ventral tegmental area. Science. 2008; 319(5867):1264–1267. [PubMed: 18309087]

Delgado MR. Reward Related Responses in the Human Striatum. Annals of the New York Academy of Sciences. 2007; 1104(1):70–88. [PubMed: 17344522]

Dolcos F, McCarthy G. Brain systems mediating cognitive interference by emotional distraction. Journal of Neuroscience. 2006; 26(7):2072–2079. [PubMed: 16481440]

Engelmann JB, Damaraju EC, Padmala S, Pessoa L. Combined effects of attention and motivation on visual task performance: Transient and sustained motivational effects. Frontiers in Human Neuroscience. 2009; 3(4)10.3389/neuro.3309.3004.2009

Engelmann JB, Pessoa L. Motivation sharpens exogenous spatial attention. Emotion. 2007; 7(3):668–674. [PubMed: 17683222]

Epstein R, Harris A, Stanley D, Kanwisher N. The parahippocampal place area: recognition, navigation, or encoding? Neuron. 1999; 23(1):115–125. [PubMed: 10402198]

Erthal FS, de Oliveira L, Mocaiber I, Pereira MG, Machado-Pinheiro W, Volchan E, Pessoa L. Load-dependent modulation of affective picture processing. Cognitive, Affective, & Behavioral Neuroscience. 2005; 5(4):388–395.

Haber SN, Knutson B. The reward circuit: linking primate anatomy and human imaging. Neuropsychopharmacology. 2010; 35(1):4–26.10.1038/npp.2009.129 [PubMed: 19812543]

Harsay HA, Cohen MX, Oosterhof NN, Forstmann BU, Mars RB, Ridderinkhof KR. Functional connectivity of the striatum links motivation to action control in humans. Journal of Neuroscience. 2011; 31(29):10701–10711.10.1523/jneurosci.5415-10.2011 [PubMed: 21775613]

Hartikainen KM, Ogawa KH, Knight RT. Transient interference of right hemispheric function due to automatic emotional processing. Neuropsychologia. 2000; 38(12):1576–1580. [PubMed: 11074080]

Horvitz JC. Mesolimbocortical and nigrostriatal dopamine responses to salient non-reward events. Neuroscience. 2000; 96(4):651–656. [PubMed: 10727783]

Kiss M, Driver J, Eimer M. Reward priority of visual target singletons modulates event-related potential signatures of attentional selection. Psychological Science. 2009; 20(2):245–251.10.1111/j.1467-9280.2009.02281.x [PubMed: 19175756]

Krebs RM, Boehler CN, Egner T, Woldorff MG. The neural underpinnings of how reward associations can both guide and misguide attention. Journal of Neuroscience. 2011; 31(26):9752–9759.10.1523/JNEUROSCI.0732-11.2011 [PubMed: 21715640]

Krebs RM, Boehler CN, Woldorff MG. The influence of reward associations on conflict processing in the Stroop task. Cognition. 2010; 117(3):341–347.10.1016/j.cognition.2010.08.018 [PubMed: 20864094]

Krebs RM, Boehler CN, Roberts KC, Song AW, Woldorff MG. The involvement of the dopaminergic midbrain and cortico-striatal-thalamic circuits in the integration of reward prospect and attentional task demands. Cerebral Cortex. 2012; 22(3):607–615. [PubMed: 21680848]

Kriegeskorte N, Simmons WK, Bellgowan PS, Baker CI. Circular analysis in systems neuroscience: the dangers of double dipping. Nature Neuroscience. 2009; 12(5):535–540.

Kristjansson A, Sigurjonsdottir O, Driver J. Fortune and reversals of fortune in visual search: Reward contingencies for pop-out targets affect search efficiency and target repetition effects. Attention, Perception & Psychophysics. 2010; 72(5):1229–1236.10.3758/APP.72.5.1229

LeDoux JE. Emotion circuits in the brain. Annual Review of Neuroscience. 2000; 23(1):155–184.

Leon MI, Shadlen MN. Effect of expected reward magnitude on the response of neurons in the dorsolateral prefrontal cortex of the macaque. Neuron. 1999; 24(2):415–425. [PubMed: 10571234]

Lim SL, Padmala S, Pessoa L. Segregating the significant from the mundane on a moment-to-moment basis via direct and indirect amygdala contributions. Proceedings of the National Academy of Sciences USA. 2009; 106(39):16841–16846.

Liu X, Hairston J, Schrier M, Fan J. Common and distinct networks underlying reward valence and processing stages: a meta-analysis of functional neuroimaging studies. Neuroscience and

Biobehavioral Reviews. 2011; 35(5):1219–1236.10.1016/j.neubiorev.2010.12.012 [PubMed: 21185861]

Loftus GR, Masson ME. Using confidence intervals in within-subject designs. Psychonomic Bulletin & Review. 1994; 1(4):476–490. [PubMed: 24203555]

Mechias ML, Etkin A, Kalisch R. A meta-analysis of instructed fear studies: implications for conscious appraisal of threat. Neuroimage. 2010; 49(2):1760–1768.10.1016/j.neuroimage.2009.09.040 [PubMed: 19786103]

Mizuhiki T, Richmond BJ, Shidara M. Encoding of reward expectation by monkey anterior insular neurons. Journal of Neurophysiology. 2012; 107(11):2996–3007.10.1152/jn.00282.2011 [PubMed: 22402653]

Mohanty A, Gitelman DR, Small DM, Mesulam MM. The Spatial Attention Network Interacts with Limbic and Monoaminergic Systems to Modulate Motivation-Induced Attention Shifts. Cerebral Cortex. 2008; 18(11):2604–2613. [PubMed: 18308706]

Padmala S, Bauer A, Pessoa L. Negative emotion impairs conflict-driven executive control. Frontiers in Psychology. 2011; 2:192.10.3389/fpsyg.2011.00192 [PubMed: 21886635]

Padmala S, Pessoa L. Reward Reduces Conflict by Enhancing Attentional Control and Biasing Visual Cortical Processing. Journal of Cognitive Neuroscience. 2011; 23(11):3419–3432.10.1162/jocn_a_00011 [PubMed: 21452938]

Park SQ, Kahnt T, Rieskamp J, Heekeren HR. Neurobiology of value integration: when value impacts valuation. Journal of Neuroscience. 2011; 31(25):9307–9314.10.1523/jneurosci.4973-10.2011 [PubMed: 21697380]

Pessoa L. To what extent are emotional visual stimuli processed without attention and awareness? Current Opinion in Neurobiology. 2005; 15(2):188–196. [PubMed: 15831401]

Platt ML, Glimcher PW. Neural correlates of decision variables in parietal cortex. Nature. 1999; 400(6741):233–238. [PubMed: 10421364]

Redgrave P, Gurney K. The short-latency dopamine signal: a role in discovering novel actions? Nature Reviews Neuroscience. 2006; 7(12):967–975.

Redgrave P, Prescott TJ, Gurney K. Is the short-latency dopamine response too short to signal reward error? Trends in Neurosciences. 1999; 22(4):146–151. [PubMed: 10203849]

Roesch MR, Olson CR. Impact of expected reward on neuronal activity in prefrontal cortex, frontal and supplementary eye fields and premotor cortex. Journal of Neurophysiology. 2003; 90(3):1766–1789. [PubMed: 12801905]

Salamone JD. The involvement of nucleus accumbens dopamine in appetitive and aversive motivation. Behavioural Brain Research. 1994; 61(2):117–133. [PubMed: 8037860]

Salamone JD, Correa M, Farrar AM, Nunes EJ, Pardo M. Dopamine, behavioral economics, and effort. Frontiers in Behavioral Neuroscience. 2009; 3:13.10.3389/neuro.08.013.2009 [PubMed: 19826615]

Salzman CD, Paton JJ, Belova MA, Morrison SE. Flexible neural representations of value in the primate brain. Annals of the New York Academy of Sciences. 2007; 1121:336–354. [PubMed: 17872400]

Savine AC, Beck SM, Edwards BG, Chiew KS, Braver TS. Enhancement of cognitive control by approach and avoidance motivational states. Cognition & Emotion. 2010; 24(2):338–356.10.1080/02699930903381564 [PubMed: 20390042]

Schultz W, Tremblay L, Hollerman JR. Reward processing in primate orbitofrontal cortex and basal ganglia. Cerebral Cortex. 2000; 10(3):272–284. [PubMed: 10731222]

Shen YJ, Chun MM. Increases in rewards promote flexible behavior. Attention, Perception & Psychophysics. 2011; 73(3):938–952.10.3758/s13414-010-0065-7

Shidara M, Richmond BJ. Anterior cingulate: single neuronal signals related to degree of reward expectancy. Science. 2002; 296(5573):1709–1711.10.1126/science.1069504 [PubMed: 12040201]

Shima K, Tanji J. Role for cingulate motor area cells in voluntary movement selection based on reward. Science. 1998; 282(5392):1335–1338. [PubMed: 9812901]

Talairach, J.; Tournoux, P. Co-planar stereotaxis atlas of the human brain. New York: Thieme Medical; 1988.

Talmi D, Dayan P, Kiebel SJ, Frith CD, Dolan RJ. How humans integrate the prospects of pain and reward during choice. Journal of Neuroscience. 2009; 29(46):14617–14626. [PubMed: 19923294]

Vul E, Harris C, Winkielman P, Pashler H. Puzzlingly high correlations in fMRI studies of emotion, personality, and social cognition. Perspectives on Psychological Science. 2009; 4(3):274–290.

Wager TD, Keller MC, Lacey SC, Jonides J. Increased sensitivity in neuroimaging analyses using robust regression. NeuroImage. 2005; 26(1):99–113.10.1016/j.neuroimage.2005.01.011 [PubMed: 15862210]

Wilcox RR. Outlier detection. Encyclopedia of statistics in behavioral science. 2005

Zink CF, Pagnoni G, Martin-Skurski ME, Chappelow JC, Berns GS. Human striatal responses to monetary reward depend on saliency. Neuron. 2004; 42(3):509–517. [PubMed: 15134646]

Highlights

- We investigated the interactions between reward and threat during a visual task
- Behaviorally, reward counteracted the task-irrelevant threat effect
- Imaging data revealed interactions in striatum, mid-cingulate and visual cortices

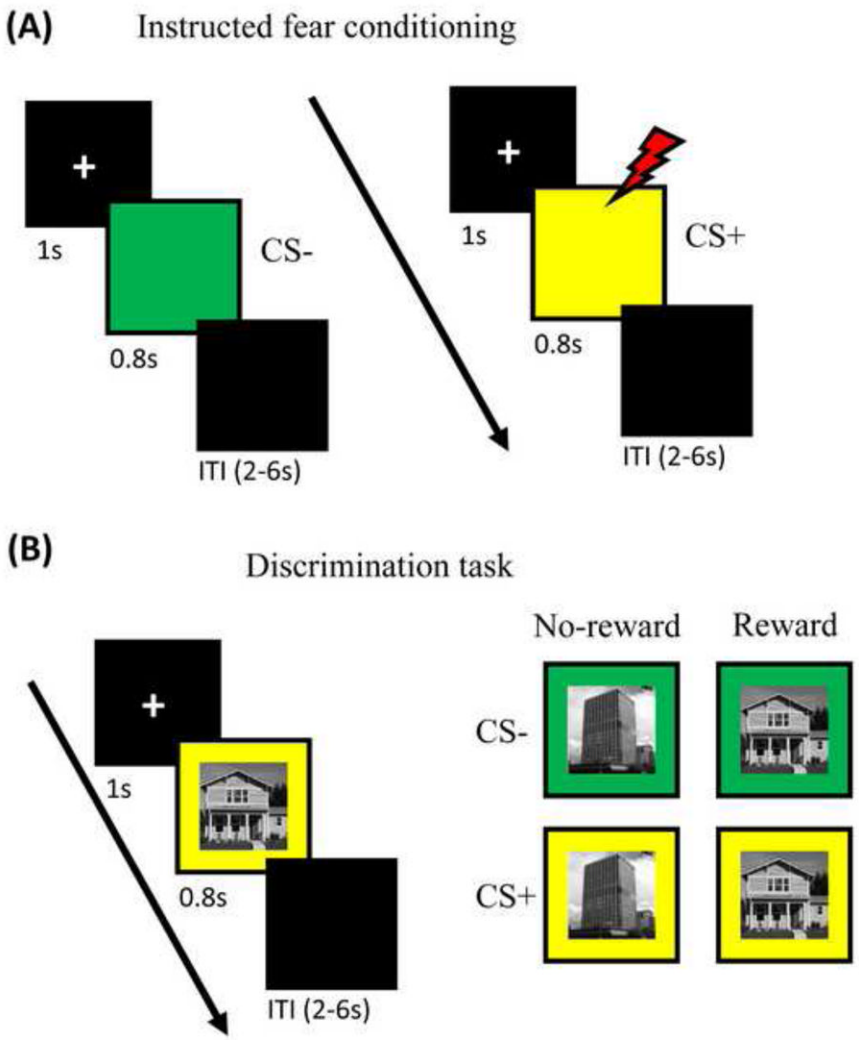

Figure 1.

Task design. (A) Instructed fear conditioning. During this phase, each trial started with an initial fixation display for 1000 msec and was followed by one of the two colored squares for 800 msec. Each trial ended with a 2-6 sec blank display. Participants passively viewed the colored square in each trial. They were explicitly informed that there was a chance of receiving a mild aversive shock when one of the colored squares appeared. Shocks (US) occurred in 50% of CS+ trials. (B) Visual discrimination task. During this phase, each trial started with an initial fixation display for 1000 msec and was followed by a picture of a house or building image overlaid on a yellow or green background for 800 msec. Each trial ended with a 2-6 sec blank display. Before the start of the experiment, participants were explicitly informed that with one of the image categories they would have the chance of winning extra monetary reward.

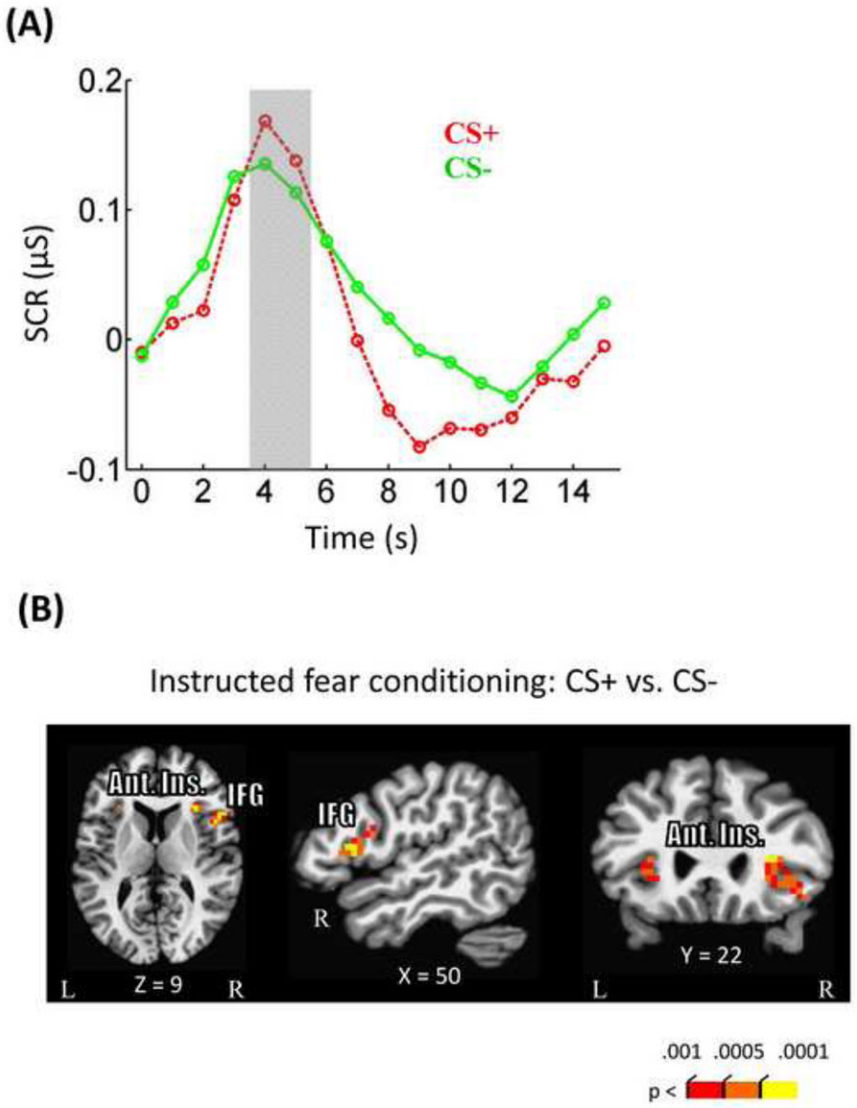

Figure 2.

Instructed fear conditioning results. (A) Stronger skin conductance responses were observed during CS+ compared to CS- trials. (B) Imaging data revealed stronger responses in CS+ compared to CS- in bilateral anterior insula, and right inferior frontal gyrus. Ant. Ins, anterior insula; IFG, inferior frontal gyrus.

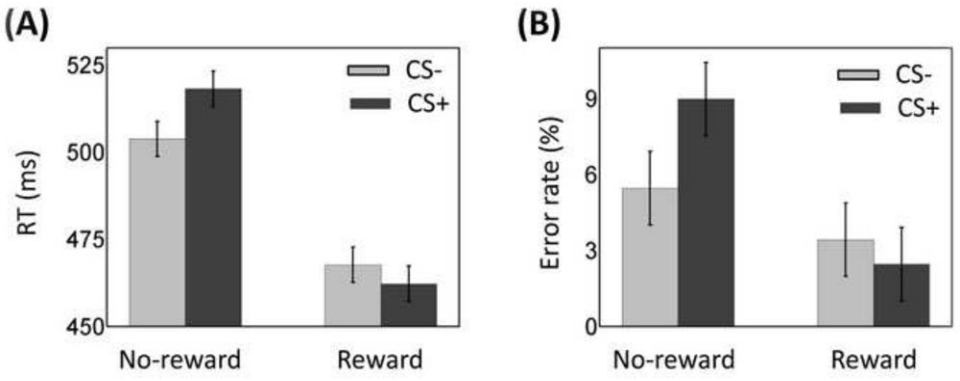

Figure 3.

Discrimination task behavioral results. (A) During no-reward trials, threat distractors slowed responses relative to safe ones. This difference was eliminated during the reward condition. (B) During no-reward trials, participants made more errors with threat distractors relative to safe ones. This difference was eliminated during the reward condition. Error bars denote the standard within-subject error term for interaction effects (Loftus & Masson, 1994).

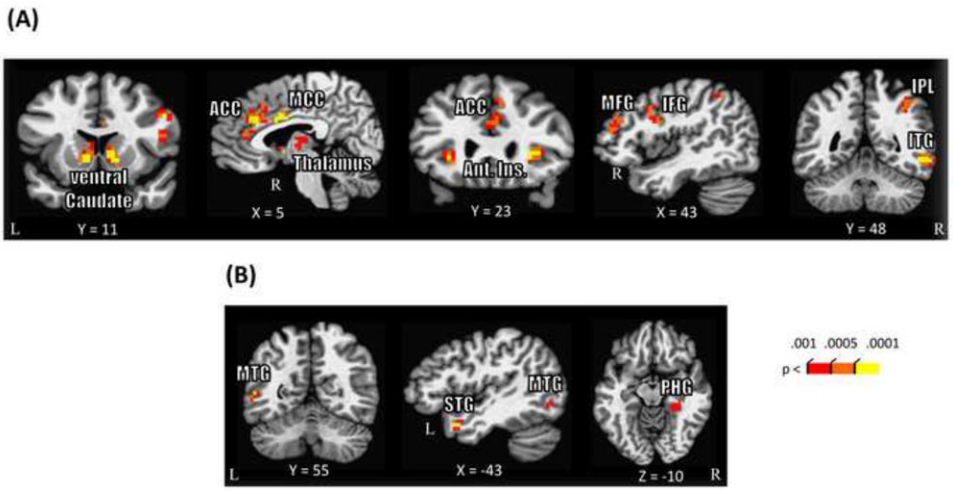

Figure 4.

Discrimination task voxelwise imaging results. (A) Regions that showed a significant main effect of Reward. (B) Regions that showed a significant main effect of Threat. The PHG cluster survived only at P < .005 (uncorrected) and 30 voxel cluster extent. Uncorrected p values are shown for display purposes (all voxels shown survived cluster-based thresholding). ACC, anterior cingulate cortex; Ant. Ins., anterior insula; MCC, mid-cingulate cortex; MFG, middle frontal gyrus; IFG, inferior frontal gyrus; IPL, inferior parietal lobule; ITG, inferior temporal gyrus; MTG, middle temporal gyrus; STG, superior temporal gyrus; PHG, parahippocampal gyrus.

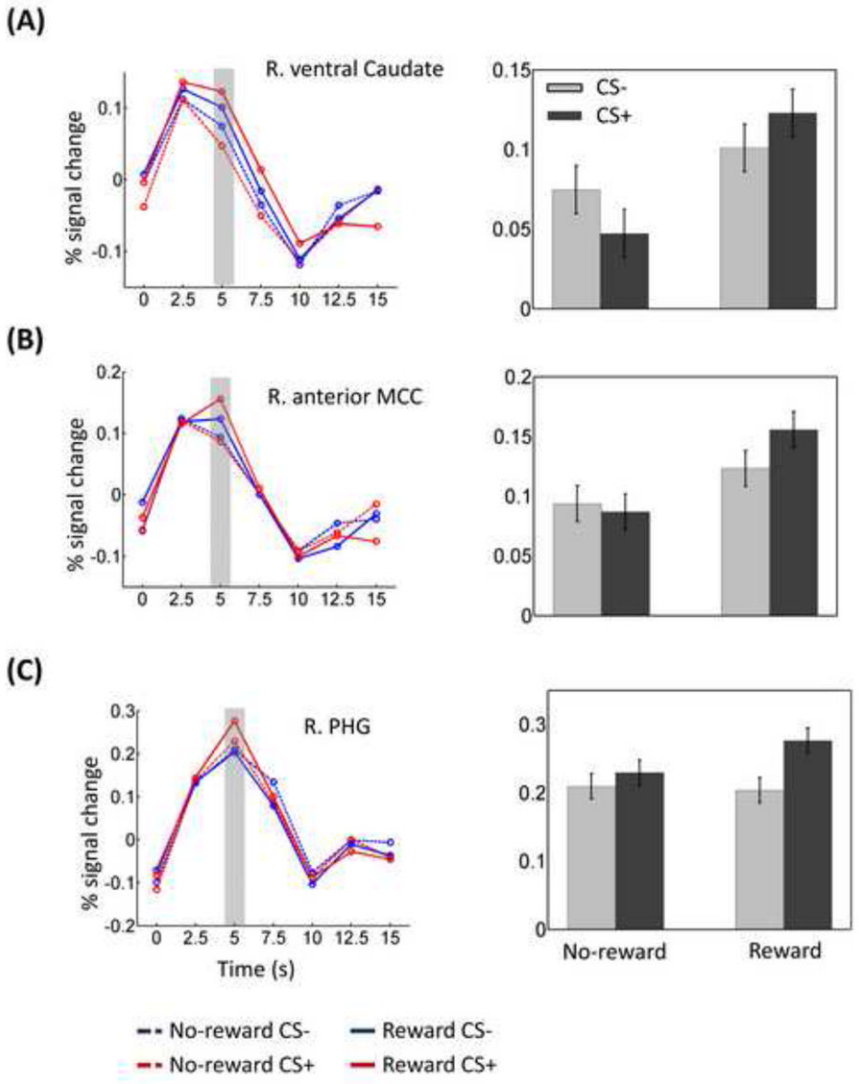

Figure 5.

Discrimination task ROI results. Average deconvolved responses and mean response indices as a function of trial type in right ventral caudate (A), right anterior mid-cingulate cortex (B), and right parahippocampal gyrus (C). The gray area indicates the time point used to index response strength. MCC, mid-cingulate cortex; PHG, parahippocampal gyrus. Error bars denote the standard within-subject error term for interaction effects (Loftus & Masson, 1994).

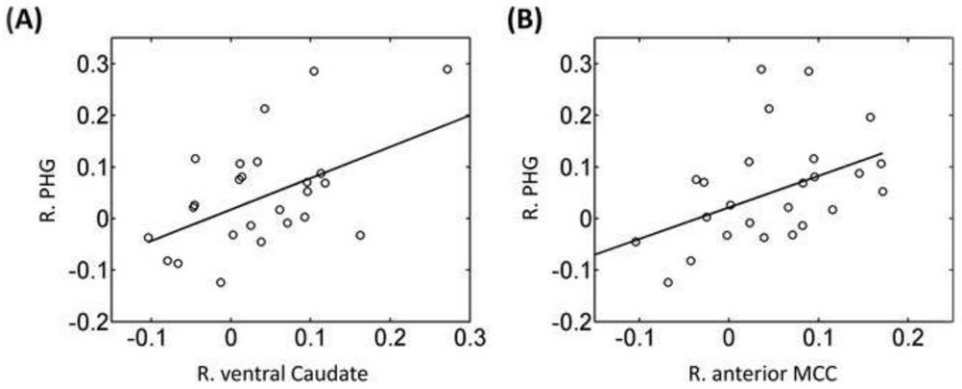

Figure 6.

Relationship between brain regions during discrimination task. Across participants, a linear relationship was observed involving fMRI interaction scores ($[CS+ – CS-]_{Reward} – [CS+ – CS-]_{No\text{-}reward}$) between right ventral caudate and right parahippocampal gyrus (A); and between right anterior mid-cingulate cortex and right parahippocampal gyrus (B).

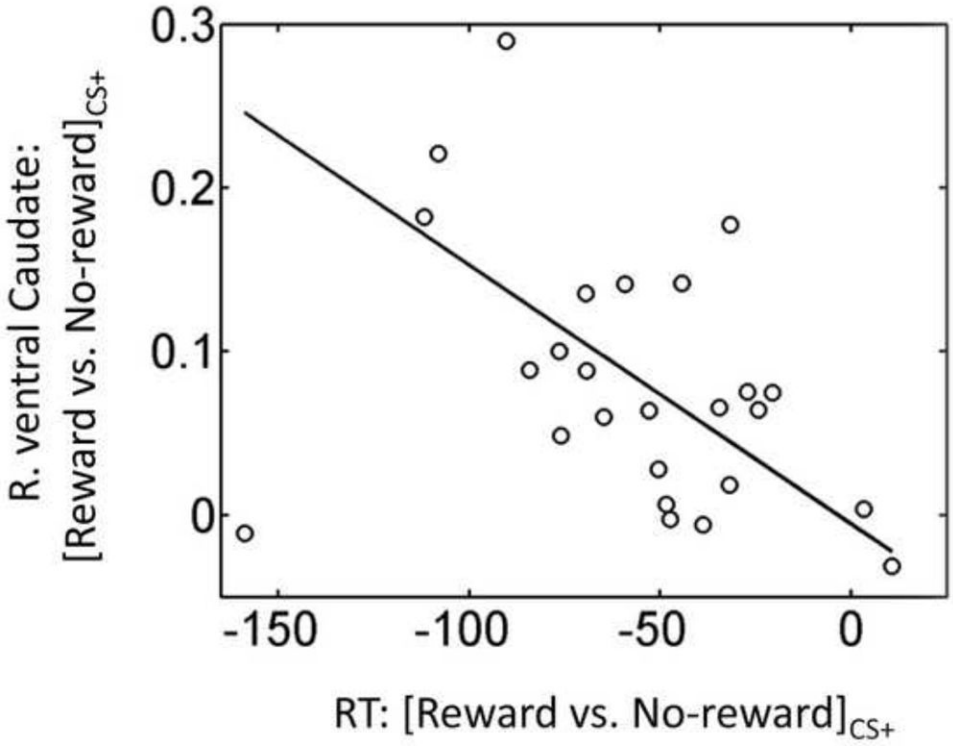

Figure 7.
Brain-behavior relationship during discrimination task. Across participants, a linear relationship was observed between differential reward vs. no-reward RT scores in the CS+ condition and corresponding differential scores in right ventral caudate.

Table 1

Instructed fear conditioning voxelwise analysis (Peak talairach coordinates, *t(25)* values and cluster size [*k*])

		CS+ vs. CS-				
Peak location		***x***	***y***	***z***	***t***	***k***
Inferior frontal gyrus	R	47	5	17	5.67	32
Anterior insula	L	-25	20	-1	4.48	22
	R	35	17	-1	5.16	87
Superior/Middle occipital gyrus	R	32	-82	26	-4.74	37

Table 2

Discrimination task voxelwise analysis (Peak talairach coordinates, *F(1,25)* values and cluster size [*k*])

		Main effect of *Reward*					Main effect of *Threat*				
Peak location		**x**	**y**	**z**	***F***	***k***	**x**	**y**	**z**	***F***	***k***
Parietal											
Inferior parietal lobule	R	32	-64	32	24.84	30					
	R	38	-52	41	21.97	27					
Temporal											
Inferior temporal gyrus	R	53	-46	-10	43.91	48					
Middle temporal gyrus	L						-49	-55	5	22.18	20
Superior temporal gyrus	L						-43	8	-22	25.64	20
Parahippocampal gyrus	R						26	-37	-10	20.75*	32
Frontal											
Anterior cingulate cortex	R	5	29	26	39.49	79					
	R	2	35	14	21.44	20					
Mid-cingulate cortex	R	5	2	29	30.89	23					
Inferior frontal/Precentral gyrus	R	47	5	23	22.90	55					
Middle frontal gyrus	R	47	41	17	29.69	49					
Anterior insula	L	-28	20	-1	28.05	29					
	R	32	23	5	31.55	39					
Subcortical											
Thalamus	R	5	-10	2	18.75	23					
Ventral caudate/nucleus accumbens	L	-4	8	2	38.11	38					
	R	11	11	-1	34.36	33					
Mid brain	L	-4	-25	-7	36.68*	37					
	R	14	-19	-7	22.17*	38					

*survived at P < .005 (uncorrected) and 30 voxel cluster extent

Table 3

ROI analysis in Amygdala

ROI	Left Amygdala		Right Amygdala	
	F(1,25)	***p***	***F(1,25)***	***p***
Main effect of *Reward*	0.006	0.940	0.960	0.337
Main effect of *Threat*	3.475	0.074	2.897	0.101
Reward × Threat	0.119	0.733	0.001	0.975